Confocal Imaging of Peripheral Regions of Intact Rat Lungs Following Intratracheal Administration of 6-Carboxyfluorescein, FITC-Insulin, and FITC-Dextran

Roderike Pohl,[1] Roger S. Thrall,[2] Rick A. Rogers,[3] and Paul A. Kramer[1,4]

Received July 10, 1998; accepted November 17, 1998

Purpose. This study compared the pulmonary disposition of 3 structurally diverse probe molecules following their intratracheal (*i.t.*) administration to anesthetized rats.

Methods. Following administration of 6-carboxyfluorescein (CF), FITC-insulin (FI) and FITC-dextran (FD), lungs were removed, inflated, perfused with a marker dye, and peripheral elements examined with confocal microscopy (CLSFM).

Results. At 5 min most of each probe remained within airspaces; the remainder distributed to interstitium, capillaries, Type II cells, and macrophages. At 60 min disposition differed significantly among probes. The smallest (CF, 376 Da) had almost completely exited airspaces and was found primarily in extracellular interstitial spaces, often behind Type II cells. Disposition was consistent with both entry into peripheral lymphatics and association with peripheral fibers. FI and FD (6 and 10 kDa, respectively) were retained substantially longer within airspaces. In contrast to CF, FI appeared to localize along septal and peripheral fibers, but its disposition was inconsistent with the involvement of peripheral lymphatics.

Conclusions. While all probes were ≤10 kDa, there was considerable disparity among both their rates of absorption and subsequent disposition within peri-alveolar elements. CLSFM appears to be a useful ancillary tool for studying the pulmonary absorption of drugs and macromolecules.

KEY WORDS: confocal microscopy; pulmonary disposition; insulin; dextran; 6-carboxyfluorescein.

INTRODUCTION

The lung is surprisingly permeable to many therapeutic peptides and proteins. Thus, pulmonary delivery offers a potential solution to the problem of developing an efficient, noninvasive route of administration that would minimize the degradation and poor systemic bioavailability characteristic of conventional routes (1,2). In conjunction with the development of strategies for peptide delivery to the systemic circulation via alveolar regions of the lung, it is desirable to characterize underlying pulmonary absorptive pathways and mechanisms.

Macromolecules introduced into alveoli by instillation or aerosolization must traverse numerous barriers including the alveolar epithelium, capillary endothelium and their associated basement membranes in order to reach the systemic circulation. Passage through the epithelium is often considered the most likely rate-limiting step and may involve transcytotic movement through cells, paracellular diffusion through the tight junctions, or osmotically driven bulk flow of solution through pores in the alveolar epithelium. While macromolecules having diameters <5–6 nm (e.g., insulin, 2.2 nm (3)) are absorbed in a matter of minutes following their intratracheal (*i.t.*) administration to animals (4,5), larger molecules exhibit considerably slower pulmonary absorption (hrs to days) (1,6).

Recently, confocal laser scanning fluorescence microscopy (CLSFM) techniques have been developed that permit *ex-vivo* imaging of sub-pleural alveoli, adjoining capillaries and lymphatic vessels, and connective tissue in intact, unfixed rat lungs. Since specimens are sectioned optically rather than physically, dehydration is unnecessary and fluids within the parenchyma and blood vessels are undisturbed (7). The lipophilic dye rhodamine B (RB) has been shown to provide a useful means of highlighting airspace and epithelial interfaces as well as such regions of interest (ROI) as capillaries, Type II alveolar epithelial cells and macrophages. Using the image registration and dual channel capabilities of CLSFM, fluorescence emissions from fluorescein-labeled molecules excited by a 488 nm laser were superimposed upon those resulting from the excitation of RB at 568 nm in order to show which structural elements of the lung were involved with various probes.

Three fluoresceinated probes, a relatively small paracellular marker (6carboxyfluorescein, CF), a polypeptide (FITC-insulin, FI), and a polysaccharide (FITC-dextran, FD), were compared with respect to their absorption from, and disposition within, peripheral lung following *i.t.* administration to anesthetized rats.

MATERIALS

Instrumentation

Fluorescent images of intact lungs were obtained using an inverted confocal microscope (Zeiss Axiovert, Model 410), equipped with Zeiss LSM software, an argon/krypton laser, and a C-Apochromat® 40x/1.2 W Korr. water-immersion objective lens. Water was used as the immersion fluid since its index of refraction approximated that of lung tissue, thereby reducing spherical aberration and increasing resolving power.

Animals and Reagents

Fischer-344 pathogen-free male rats (175–225 g) were obtained from Charles River Laboratories, Kingston, RI. Rhodamine B (RB; Eastman Kodak, Rochester, NY), 6-carboxyfluorescein (CF; Molecular Probes, Eugene, Oregon), FITC-insulin (FI; Sigma, St. Louis, MO) and FITC-dextran (FD, 10 kDa; Sigma, St. Louis, MO) were used without further purification. Modified lactated Ringer's solution consisted of lactated Ringer's (Baxter Corp. Deerfield, IL) supplemented with 0.005 M Na_2PO_4 and 5.37 mM NaCl (285 mOsmol/L, pH 7.4).

[1] Department of Pharmaceutical Sciences, School of Pharmacy, Storrs, Connecticut 06268.
[2] Departments of Medicine and Surgery, University of Connecticut Health Center, Farmington, Connecticut 06030.
[3] Department of Physiology, Harvard School of Public Health, Boston, Massachusetts 02115.
[4] To whom correspondence should be addressed. (e-mail: kramer@nso2.uchc.edu)

0724-8741/99/0200-0327$16.00/0

METHODS

Confocal Microscopy

Intratracheal Instillation of Fluorescent Probes to Rats

Rats were anesthetized with ketamine (80 mg/kg)/xylazine (10 mg/kg), secured at a 30° angle from horizontal and the trachea exposed. A small incision was made between the fifth and sixth tracheal rings and a cannula (PE-90) inserted into the respiratory tract to a depth of 3.5 cm. For each probe studied, 4 rats were temporarily tilted to an 85° angle and 0.1 ml of probe, dissolved in phosphate-buffered saline (pH 7.4, 4.5 nanoequivalents fluorescein) were introduced over 30 sec, followed by a 0.2 ml air bolus to clear the cannula of residual fluid. The cannula was promptly removed, and rats returned to their original horizontal position (1 min post injection). An endotracheal tube was secured into the trachea to maintain airflow and a heat lamp used to maintain body temperature at 37°C during the absorption period.

Lung Preparation for Microscopy

At various pre-determined times (5, 30, 60, 120 and 240 min), rats were exsanguinated and the thoracic cavity opened. Heparin (1000 U in 0.1ml) was injected into the right side of the heart (still beating) and allowed to circulate for one min. The lungs, with heart still attached, were carefully excised, and placed in a petri dish. The lower portion of the heart was removed, exposing the left and right ventricles, and a cannula inserted into the pulmonary artery *via* the right ventricle. The lungs were inflated with air through the endotracheal tube and maintained at 60% of total lung capacity (15 cm water pressure).

The lungs were perfused by gravity feeding modified lactated Ringer's solution (15 cm water pressure) in through the pulmonary arterial cannula and out *via* the left atrium. When most erythrocytes had been flushed from the vasculature, the perfusate was supplemented with RB (10 μg/ml). Perfusion was terminated when RB was visible in the effluent.

Confocal Setup

The inflated lungs were placed heart side down within a specially designed chamber, consisting of a 55 mm petri dish adapted for microscopy by replacing a rectangular portion of its bottom with a 20 × 40 mm (#1$\frac{1}{2}$) glass coverslip (7). Images produced by the 488 nm excitation laser had settings for pinhole and attenuation of 30, while those using 568 nm excitation had pinhole and attenuation set at 40 and 10, respectively. Contrast and brightness settings were extended to a full intensity range (grayscale) of 0–255 before imaging each preparation.

Image Acquisition

Laser excitation wavelengths of 488 nm and 568 nm were used individually to scan lung tissue, and fluorescent emissions from CF, FI, FD (emission λ = 515–545 nm), and RB (emission $\lambda > 630$ nm) were collected using separate channels. Grayscale images (obtained from each scan) were pseudo-colored green (CF, FI, FD) and red (RB) then overlaid (Zeiss LSM confocal software) to form a multicolored image.

Data on the relative fluorescence of CF, FI and FD within various ROI were obtained from within a series of five image fields per rat. Uniform image depth was accomplished by initially focusing the laser on the inside edge of the peripheral fiber network of the left lobe of the lung, then re-focusing the laser 10 μm further into the lung. The original image field (159 μm^2) was centered in a region of probe fluorescence containing numerous alveoli, ignoring regions with a preponderance of connective tissue elements, larger airways, etc. Attempts were made to identify areas of comparable appearance among rats to facilitate comparisons. Four additional images were taken from adjacent fields above and to the right, above and to the left, below and to the left, and below and to the right of the original field. A cross section of the edge of the lung was also included in each data set. All images were recorded within 30 minutes of animal death.

Image Analysis

Images were split into separate channels, red (RB) and green (probe), and loaded into RatioView® image analysis software (Version 1.0, CBIT, Farmington, CT). Identification of ROI (airspace, interstitium, type II cells, macrophages, and capillaries) was done by first locating the ROI on the red (RB) channel (7), and then masking the identified area. The mask was overlaid on the green channel image (probe), to identify the ROI. The average intensity and area of each mask on the

Fig. 1. (*opposite, top*) Peripheral alveolar disposition of 6-carboxyfluorescein (CF, green) in intact, fully-hydrated, rhodamine-stained (red) lungs at various times following intratracheal instillation of CF into anesthetized rats. Dark, non-fluorescent areas of all images are pockets of air within alveoli. Five minutes after administration CF remains largely within the airspaces (1a). Images 1b, 1c and 1d (taken after 30, 60 and 120 min. of absorption, respectively) show the disappearance of CF from those airspaces, penetration around epithelial cells (1b, arrow) and appearance in the interstitium in the vicinity of Type II cells (1c, arrows). These 4 confocal microscopy images were taken at a depth of 10 μm into the lung parenchyma measured from the inner edge of the peripheral fiber network. Images of the outer periphery of the lung taken at 60 and 120 min. post-instillation (1e, 1f, respectively) show CF filling what appear to be peripheral lymphatic vessels (*) and staining the peripheral fiber network (arrow).

Fig. 2. (*opposite bottom*) Peripheral alveolar disposition of FITC-insulin (FI; 2a & 2b) and FITC-dextran (FD; 2d & 2e) in intact, fully-hydrated, rhodamine-stained (red) rat lungs 5 and 60 min (2a, 2d and 2b, 2e respectively) after their intratracheal instillation into anesthetized rats. These 4 confocal microscopy images were taken at a depth of 10 μm into the lung parenchyma measured from the inner edge of the peripheral fiber network. Dark non-fluorescent areas are pockets of air within alveoli. Five minutes after administration, both FI and FD remained largely within the airspaces. At 60 min, FI appears to be fluorescing along septal fibers within the interstitium (2b, arrow), while FD remains confined to the airspaces (2e). Images of the outer periphery of the lung (taken at 60 min post-instillation), show FI staining peripheral fibers (2c, arrow), in contrast to a lack of such staining for FD (2f, arrow).

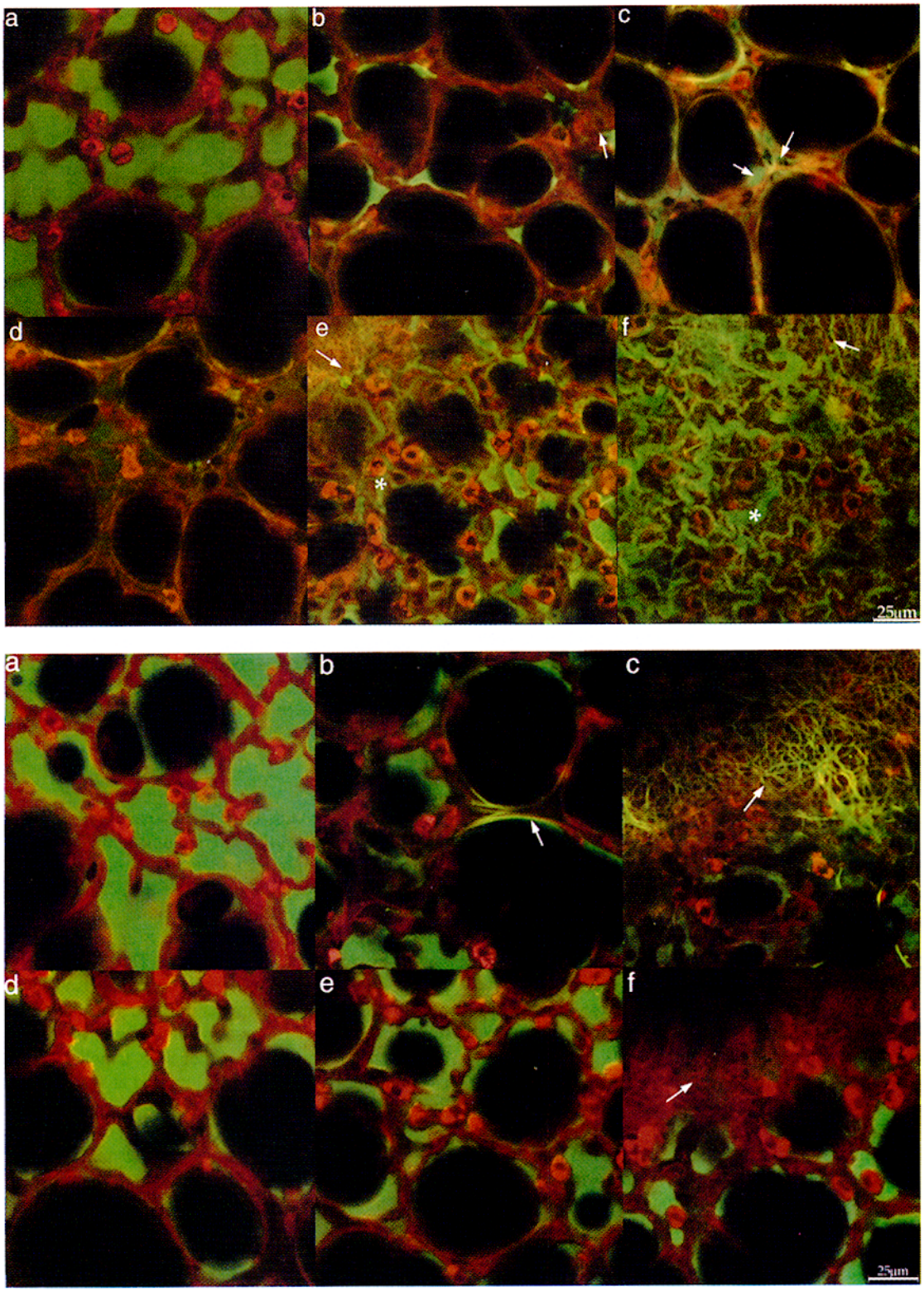
a
b
c
d
e
f
25μm
a
b
c
d
e
f
25μm

Table I. Time Course of Interalveolar Septal Thickness Following Intratracheal Administration of 6-carboxyfluorescein[a] to Rats

Time (min.)	Mean septal thickness[b]	Standard deviation	P value[c]
5 min	6.2	1.6	
30 min	6.6	2.2	0.4564
60 min	8.3	2.9	0.0018
120 min	11.5	6.3	0.0000
240 min	10.0	4.3	0.0008

[a] Dose = 4.5 nanoequivalents of 6-CF.
[b] 5 measurements/image × 5 images/rat × 4 rats.
[c] Compared to previous timepoint.

green channel was calculated and recorded. Fraction of total fluorescence in each ROI was calculated by dividing the fluorescence from each ROI ([area in pixels] × [average intensity per pixel]) by the total fluorescence ([total area in pixels] × [average intensity per pixel]) for each data set of five image fields (n = 4 sets/time period). Background fluorescence was subtracted from each image prior to analysis.

Thicknesses of inter-alveolar septa were measured for images taken 5, 30, 60, 120, and 240 min. post intratracheal instillation of CF. The dimension used was the distance between the epithelial surfaces of two adjoining airspaces at the point where tangent lines to each surface became parallel. Five such measurements were made per image, (5 images/rat, and 4 rats/time period) for a total of 100 measurements per time period. A single-factor ANOVA with stepwise comparisons (least significant difference method) was used to test for differences among the mean values as time progressed (STAN©, Version II, Statistical Consultants, Inc., 1984).

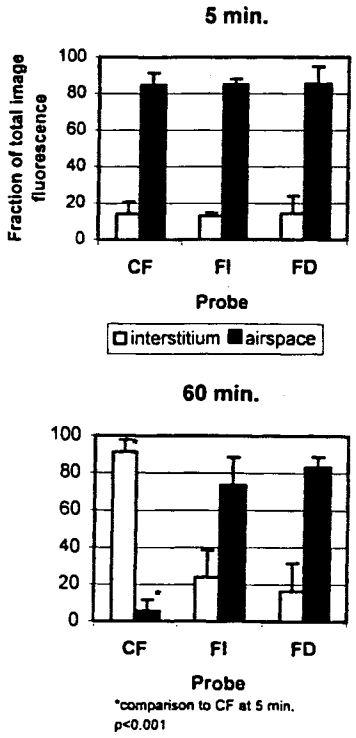

Fig. 3. Fraction of total confocal image fluorescence present in pulmonary airspaces and interstitium for each of 3 fluorescent probes (6-carboxyfluorescein, CF; FITC-insulin, FI; and 10 kDa FITC-dextran, FD). Left and right panels show results at 5 min and 60 min, respectively, after intratracheal administration of probes (measured as 4.5 nanoequivalents of fluorescein).

RESULTS

Representative confocal images of the peripheral alveolar disposition of CF (green) in intact, fully hydrated rhodamine-stained lungs (red) are shown in Fig. 1. Figure 3 summarizes a semi-quantitative assessment of probe movement, expressed as percentage of total probe within an image field that was located within either airspaces or interstitial regions.

The first 4 images of Fig. 1, taken 10 μm toward the lung parenchyma from the inner edge of the peripheral fiber network, show *in vivo* absorption of CF after 5, 30, 60, or 120 min in anesthetized rats (Figs. 1a–1d, respectively). Five min after instillation, ~85% of the probe molecules within the visual field were within the airspaces (Fig. 1a). Within 30 min, CF had penetrated the alveolar epithelium, and moved into "free" (i.e., extracellular) interstitial spaces (Fig. 1b, arrow). Images appeared to show CF in punctate regions between cells. It is evident qualitatively in Fig. 1c and semi-quantitatively in Fig. 3 that at 60 min, CF had almost completely relocated from the alveolar airspaces to interstitial spaces, localizing in areas of intense fluorescence within the interstitium. Images at later absorption times (e.g., 120 min) revealed what appeared to be a thickened alveolar septa (Table I), with CF fluorescence distributed more uniformly than at earlier times (Fig. 1d). Quantitative measurement confirmed a statistically significant ($p < 0.05$) increase in septal thickness over time with a maximum at 120 min post-dose. Beyond that there was a significant, albeit modest, decrease in septal thickness by 240 min.

To further characterize the dispositional course of CF following its arrival in the interstitium, optical cross sections of the peripheral lung after an absorption period of 1 hr (Fig. 1e) and, specifically, regions just inside the peripheral fiber network (Fig. 1f, after an absorption period of 2 hr) were examined. These images showed CF filling what appeared to be peripheral lymphatic vessels (Fig. 1e, 1f, *). These vessels merge with peripheral fibers (Fig. 1e, 1f, arrow) which also became fluorescent in regions where lymphatics (rendered fluorescent because of their content of CF) are in contact with them. Type II cells had not taken up CF into either their lamellar bodies or cytoplasm, nor did macrophages fluoresce at any of the absorption times studied.

The peripheral alveolar disposition of both macromolecular probes (FI and FD) was also determined in intact, fully-hydrated rat lungs 5 and 60 min after *i.t.* instillation for comparison both with each other and with the far smaller CF probe molecule. Like CF, both were largely (~85% of total image fluorescence) constrained to the airspaces at 5 min post-administration (Figs. 2 and 3). For all three probes, a small amount of probe fluorescence was found within the interstitium at 5 min post-administration. After 60 min of absorption, little had changed with respect to either the airspace or interstitial fluorescence of FD (Figs. 2d and 2e), while additional, albeit statistically insignificant ($p = 0.33$), amounts of FI fluorescence had exited the airspaces and appeared in the interstitium (Fig. 3). A corresponding decline in FI fluorescence in the airspaces between 5 and 60 min. was also not significant ($p = 0.27$).

Specific images do confirm, however, a considerable "drying" of the airspaces over that period (Figs 2a and 2b), a phenomena that was not seen for FD (Figs 2d and 2e). Instead of being distributed within free interstitial space as was CF, FI fluorescence was associated with parenchymal fibers, which it rendered intensely fluorescent (Fig. 2b, arrow). Peripheral lymphatics, clearly illuminated by CF (Fig. 1e, 1f, *) were not similarly evident here (Fig. 2c, arrow). In spite of this, FI reached the outer peripheral fiber network.

DISCUSSION

CF, FI and FD displayed widely disparate absorption and disposition characteristics over a 2 hr period following their instillation as buffered, aqueous solutions into subpleural alveoli. The smallest, CF, which has been shown to penetrate paracellularly through both ocular and buccal epithelia and as well as frog cerebral microvessels (8), left the airspaces most rapidly and accumulated in the extracellular regions of the interstitium behind Type II epithelial cells. This is the region where Walker has postulated that 3 alveoli in close apposition may form a "trijunctional pore" (nominal diameter as large as 27 nm, (9)). In contrast to paracellular diffusion, passage through such pores could involve an osmotically driven convective process wherein water accompanies the movement of CF into interstitial spaces that might distend as a result (1). The speed of its appearance in the interstitium (Fig. 3) would be consistent with such a movement of probe solution rather than probe diffusion across the alveolar epithelium. In addition, the data in Table I provide some support for the notion that the interstitium did indeed expand as CF appeared within it, perhaps because of solvent (water) accompanying the movement of probe molecules.

Both FI and FD solutions seemed to disappear from subpleural alveolar airspaces considerably more slowly than CF. While the equivalent sphere diameter of monomeric insulin is 2.2 nm (3), the molecule might be expected to exist primarily as a dimeric association complex at physiological pH (10). As long as the FITC derivatization did not affect its association properties (and we do not know that it didn't), FI would be comparable in size to FD (4.4 nm (11)), perhaps explaining the observed similarities in the intra-alveolar appearances of the two probes at 5 and 60 min. The slow egress of FD from the airspaces also consistent with the findings of both Morita (12) and our Laboratory (Pohl, 1998 unpublished) which, based on deconvolution of systemic plasma levels, indicated FD is absorbed approximately 20 times more slowly than CF following their intratracheal dosing to anesthetized rats.

In addition, the images in Fig. 2 show that peripheral alveoli, filled with probe solution, appeared to "dry" much more slowly when FD was the solute than when FI was involved. The capacity of FD to hydrogen bond to water (dextrans are used clinically as plasma expanders) could account for such differences in the rate of loss of water from the airspaces.

The peripheral alveolar disposition of CF and FI also differed. CF appeared to enter the lymph-like extracellular fluid of the interstitium as a prelude to subsequent "downstream" involvement with alveolar capillaries, peripheral lymphatics and fibrous elements of the connective tissue network, which pervades the entire lung from hilus to the pleural surface (13). This extracellular fluid is continually drained toward the pleural surface of the lung via the peripheral lymphatics or toward juxta-alveolar lymphatics deeper within the parenchyma.

In contrast to CF, rather than occupy extracellular fluid spaces within the interstitium, FI appeared to associate with its fiber network. While the resulting "striated" appearance of FI within the interstitium only suggests a possible interaction with parenchymal/septal fibers, a possible explanation is the binding of FI to them. Fibrous components of the peripheral fiber network include collagen and elastin as well as heparin and chondroitin sulfates. The latter can take up large amounts of water and potentially associate with solutes like those administered in this study. Dadey has recently reported an association between insulin and low MW heparins (14).

Thus, in spite of the fact that all probes studied were relatively small ($\leq$10 kDa), there was considerable disparity among them with respect to both their disappearance from alveolar airspaces and subsequent disposition within perialveolar elements.

Our results indicate that CLSFM, when used creatively with pharmacokinetic techniques, other microscopies and, perhaps immunochemical techniques, may prove to be a useful ancillary tool for studying the pulmonary deposition, absorption and subsequent disposition of drugs and macromolecules in the peripheral lung. In spite of its limited resolution, it should be useful for examining such phenomena as the deposition of dry powder protein/peptide formulations and macromolecular aggregation induced by interactions with pulmonary surfactant.

ACKNOWLEDGMENTS

The authors would like to thank Dr. John Patton (Inhale Therapeutic Systems Inc) for assistance throughout the project; and Mr. Frank Morgan, Ms. Sue Krueger and Dr. Ann Cowan (Center for Biomedical Imaging Technologies) for their assistance with CLSFM. The financial support of the Pharmaceutical Research and Manufacturers of America, Inhale Therapeutic Systems Inc, and the University of Connecticut Research Foundation are also gratefully acknowledged.

REFERENCES

1. J. Patton. Mechanisms of macromolecule absorption by the lungs. *Adv. Drug Del. Rev.* **19**:3–36 (1996).
2. P. Byron and J. Patton. Drug delivery via the respiratory tract. *J. Aerosol Med.* **7**:49–75 (1994).
3. H. Olesen, J. Rehfeld, B. Hom, and E. Hippe. Stokes radius of ^{57}Co-labelled vitamin B_{12}-transcobalamin I and II and ^{125}I-labelled insulin estimated by Sephadex G-200 gel filtration in human plasma at 37°. *Biochim. Biophys. Acta* **194**:67–70 (1969).
4. P. Colthorpe, S. Farr, G. Taylor, I. Smith, and D. Wyatt. The pharmacokinetics of pulmonary-delivered insulin: A comparison of intratracheal and aerosol administration to the rabbit. *Pharm. Res.* **9**:764–768 (1992).
5. R. Niven, F. Lott, and J. Cribbs. Pulmonary absorption of recombinant methionyl human granulocyte colony stimulating factor (r-huG-CSF) after intratracheal instillation to the hamster. *Pharm. Res.* **10**:1604–1610 (1993).
6. R. Hastings, M. Grady, T. Sakuma, and M. Matthay. Clearance

of different-sized proteins from the alveolar space in humans and rabbits. *J. Appl. Phys.* **73**:1310–1316 (1992).
7. R. Pohl, P. Kramer, and R. Thrall. Confocal laser scanning fluorescence microscopy of intact rat lungs. *Int. J. Pharm.* **168**:69–77 (1998).
8. P. Fraser and A. Dallas. Permeability of disrupted cerebral microvessels in the frog. *J. Phys.* **461**:619–632 (1993).
9. D. Walker, A. MacKenzie, W. Hulbert, and J. Hogg. A reassessment of the tricellular region of epithelial cell tight junctions in trachea of guinea pig. *Acta Anat.* **122**:35–38 (1985).
10. B. Frank, A. Pekar, and A. Veros. Insulin and proinsulin conformation in solution. *Diabetes* **21**:486–491 (1972).
11. R. Chang, I. Ueki, J. Troy, W. Deen, C. Robinson, and B. Brenner. Permselectivity of the glomerular capillary wall to macromolecules, II. Experimental studies in rats using neutral dextran. *Biophys. J.* 15 (1975).
12. T. Morita, A. Yamamoto, M. Hashida, and H. Sezaki. Effects of various absorption promoters on pulmonary absorption of drugs with different molecular weights. *Biol. Pharm. Bull* **16**:259–262 (1993).
13. E. Weibel and R. Crystal. Structural organization of the pulmonary interstitium. In: *The Lung: Scientific Foundations* (second ed.), edited by R. Crystal and J. West. Philadelphia: Raven Publishers, 1997, p. 685–695.
14. E. Dadey. Effect of pH and polyelectrolyte concentration on the aggregation state of insulin. *Pharm. Res.* **14**:S-495 (1997).